

## A Linear Muffin-Tin Orbital Calculation of Local Electronic and Magnetic Properties of $\text{YFe}_{10}\text{Mo}_2$ and $\text{YFe}_{10}\text{Mo}_2\text{N}$

Jinbo YANG, Bo CUI, Weihua MAO, Yingchang YANG,  
Dongfeng CHEN<sup>1</sup>, Jilian YANG<sup>1</sup> and Cheng GOU<sup>1</sup>

*Department of Physics, Peking University, Beijing 100871, P. R. China*

<sup>1</sup>*Institute of Atomic Energy, Academic Sinica, Beijing 102413, P. R. China*

(Received May 30, 1997)

Structure and magnetic properties of  $\text{YFe}_{10}\text{Mo}_2$  and  $\text{YFe}_{10}\text{Mo}_2\text{N}$  compounds have been studied with neutron diffraction and self-consistent spin-polarized linear muffin-tin orbital (LMTO) band calculation. The diffraction results indicate that the nitrogen atoms are located at 2b sites with nearly 99% occupancy. The electronic structure calculations give excellent results for site-dependent Fe magnetic moments and hyperfine fields. The interstitial-atom effect on the local magnetic moments and hyperfine fields is explained with magneto-volume effect and chemical bonding effect. The contributions of the magneto-volume effect and the chemical bonding effect of the nitrogen to the magnetic moments ( $\mu_{Loc}$ ), Fermi-contact hyperfine fields ( $H_{FC}$ ) and isomer shifts ( $IS$ ) are reported.

KEYWORDS: the LMTO method, band calculation,  $\text{YFe}_{10}\text{Mo}_2$ ,  $\text{YFe}_{10}\text{Mo}_2\text{N}$ , magnetic moments, hyperfine interaction, neutron diffraction

### §1. Introduction

Recently, the interstitial modified intermetallic materials based on rare earth (R) and iron have been studied quite intensively, especially since the discoveries of the  $\text{R}_2\text{Fe}_{17}\text{N}_x$ <sup>1)</sup> and  $\text{RFe}_{11}\text{TiN}_x$ .<sup>2)</sup> It has shown that by introducing the nitrogen atoms into crystallographic lattice, the Curie temperature ( $T_c$ ) was found to be increased by 400 K on the average over the rare earth series  $\text{R}_2\text{Fe}_{17}$ <sup>3)</sup> and about 200 K for  $\text{R}(\text{Fe}, \text{M})_{12}$  ( $\text{M}=\text{Ti}, \text{V}, \text{Mo}, \text{W}, \text{etc.}$ ) compounds. The Fe magnetic moments were increased by 10–20% in 1:12 (ThMn<sub>12</sub> type) nitrides.<sup>4)</sup> In addition, the crystal environment of the rare earth atoms was also significantly modified, resulting in a strong easy-axis anisotropy at room temperature for  $\text{Sm}_2\text{Fe}_{17}\text{N}_x$  and  $\text{R}(\text{Fe}, \text{M})_{12}\text{N}_x$  when  $\text{R}=\text{Nd}, \text{Pr}, \text{Tb}, \text{Dy}$  and  $\text{Ho}$ . So far the increase of the  $T_c$  and the magnetic moments have been regarded as being attributed to the interstitial doping.

It is thereby assumed generally that the following two effects are responsible for the modification of the properties after interstitial doping:<sup>5-10)</sup> (a) The magneto-volume effect, due to the increase of the crystal unit cell volume. (b) The chemical bonding effect, due to the charge transfer and hybridization between the interstitial atoms and the neighbor atoms. Experimentally, these two effects can hardly be separated.

To clarify the origin of the improvement of these magnetic properties, band calculation have been performed for these intermetallic compound. Several authors have made band calculations on the  $\text{R}(\text{Fe}, \text{M})_{12}$  ( $\text{M}=\text{Mo}, \text{V}, \text{Ti}$ )<sup>11, 12)</sup> and  $\text{RFe}_{12}$ .<sup>13)</sup> In most of these calculations, however, experimental data of true crystallographic structure are not used. The studies of the nitrides are mainly focused on  $\text{YFe}_{11}\text{TiN}$ <sup>9, 10, 14)</sup> with true

experimental structure parameters. Asano *et al.*<sup>15)</sup> and Ishida *et al.*<sup>16)</sup> have studied the electronic structure of  $\text{YFe}_{12}\text{N}$  and  $\text{YFe}_{12-x}\text{Mo}_x\text{N}$  with a hypothetical structure parameters.

However, the question of the interstitial atoms effect in 1:12 nitrides is still an object of controversy. Li and Coey<sup>9)</sup> have suggested that the enhancement of the magnetic moment is sum of a positive contribution due to volume effect and a negative contribution due to nitrogen insertion. Sakuma<sup>10)</sup> suggested that the N atoms enhance the Fe moments not only through magneto-volume effect but also by changing the electronic bonding nature. To date, the details about the nitrogen effect on different Fe sites of 1:12 nitrides are not clearly understood.

Furthermore, the hyperfine field ( $HF$ ) and isomer shift ( $IS$ ) are two important parameters of the hyperfine interaction, which depend sensitively on the properties of the ground states. A theoretical report of the hyperfine field is still lacking in 1:12 compounds. Recently, the Fermi-contact hyperfine fields ( $H_{FC}$ ) of  $\text{RFe}_{12}\text{X}$  ( $\text{R}=\text{Gd}, \text{Ce}, \text{X}=\text{C}, \text{N}$ ) were calculated.<sup>15)</sup>

In the present paper, we prepared the  $\text{YFe}_{10}\text{Mo}_2$  and  $\text{YFe}_{10}\text{Mo}_2\text{N}$  compounds, then carried out a neutron diffraction to determine the crystallographic sites of  $\text{YFe}_{10}\text{Mo}_2$  alloy and its nitride. And based on our experimental crystallographic structures, spin-polarized band calculations were performed with using the linear muffin-tin orbital (LMTO) method.<sup>17, 18)</sup> The nitrogen atoms effect on the magnetic moments and hyperfine parameters was discussed with chemical bonding effect and magneto-volume effect.

### §2. Experimental Methods

Alloy with composite of  $\text{YFe}_{10}\text{Mo}_2$  was prepared by arc-melting using 99.9% pure metals. The nitrides were

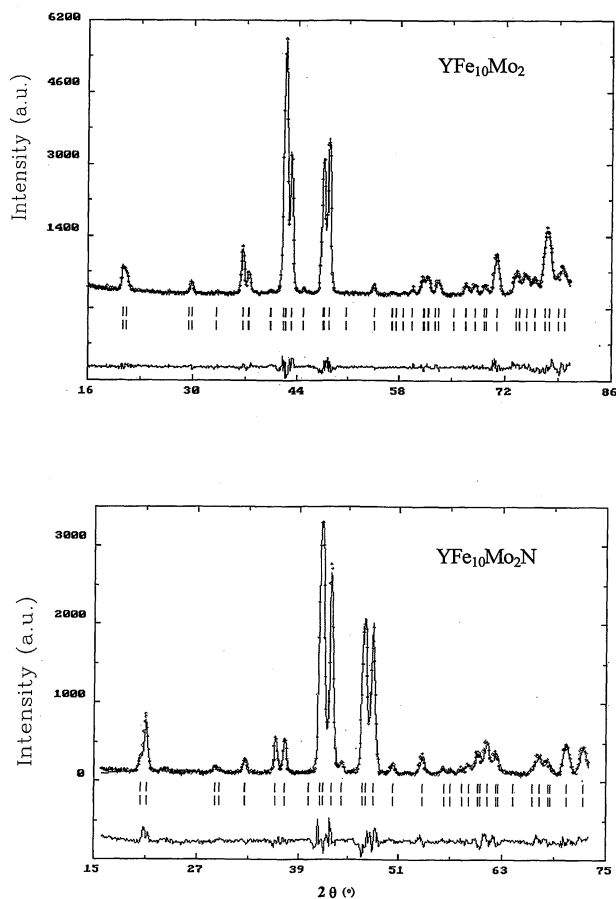


Fig. 1. The neutron diffraction patterns of  $\text{YFe}_{10}\text{Mo}_2$  and  $\text{YFe}_{10}\text{Mo}_2\text{N}$ .

formed by heating fine powder samples in approximately 1 bar of nitrogen at  $580^\circ\text{C}$  for 4 hours. Both standard X-ray diffraction with  $\text{Cu-K}\alpha$  radiation and thermomagnetic analysis were used for checking the quality of the samples. The  $\text{YFe}_{10}\text{Mo}_2$  and  $\text{YFe}_{10}\text{Mo}_2\text{N}_x$  are single phase, expect a little amount  $\alpha\text{-Fe}$  in nitrides which is inevitable in the nitrogenation process.<sup>19)</sup> Judging from the very well-defined X-ray diffraction peaks and sharp magnetic phase transition at cure temperature, we believe 1:12 Mo nitrides are the best among all the 1:12 nitrides.

In order to obtain more reliable experimental lattice constants, neutron diffraction experiments were carried out on a triple-axis spectrometer of which the analyzer is available to improve resolution and decrease inelastic background. The neutron diffraction data were analyzed by Izumi's Rietveld structure refinement program REIEAN.<sup>20)</sup> In Fig. 1, the room temperature neutron diffraction patterns of  $\text{YFe}_{10}\text{Mo}_2$  and  $\text{YFe}_{10}\text{Mo}_2\text{N}$  are presented. As shown in the figure, the nitrides retain the crystallographic symmetry of the host compounds. From Table I, the Rietveld structure analysis shows that Mo atoms occupy the 8i sites, which is consistent with most of the experiments results.<sup>19,21)</sup> N atoms are located on the 2b sites, which are the center of an octahedron formed by four Fe(8i) atoms and two Y(2a) atoms, with nearly 99% occupancy. N insertion results in an expanded lattice cell with expansion mainly along the

Table I. Refinement parameter of  $\text{YFe}_{10}\text{Mo}_2$  and  $\text{YFe}_{10}\text{Mo}_2\text{N}$  at room temperature. n is the occupation factor, x, y, z are the fractional position coordinates; m is the magnetic moment ( $\mu_B$ ). Numbers in parentheses are the statistical errors given by the refinement program.

$\text{YFe}_{10}\text{Mo}_2$					
$a=b=8.572 \text{ (\AA)} \quad c=4.809 \text{ (\AA)}$					
$R_I = 3.02\% \quad R_F = 2.47\% \quad T_c = 360 \text{ K}$					
	n	x	y	z	m
Y(2a)	1.0	0	0	0	0
Fe(8i)	0.48(1)	0.359(1)	0	0	1.3(3)
Mo(8i)	0.52(2)	0.359(1)	0	0	0
Fe(8j)	1.0	0.279(1)	0.5	0	1.3(3)
Fe(8f)	1.0	0.25	0.25	0.25	1.3(3)
$\text{YFe}_{10}\text{Mo}_2\text{N}$					
$a=b=8.694 \text{ (\AA)} \quad c=4.816 \text{ (\AA)}$					
$R_I = 3.80\% \quad R_F = 3.03\% \quad T_c = 450 \text{ K}$					
	n	x	y	z	m
Y(2a)	1.0	0	0	0	0
Fe(8i)	0.48(2)	0.360(1)	0	0	1.6(3)
Mo(8i)	0.52(2)	0.360(1)	0	0	0
Fe(8j)	1.0	0.282(1)	0.5	0	1.6(3)
Fe(8f)	1.0	0.25	0.25	0.25	1.6(3)
N(2b)	0.99(2)	0	0	0.5	0

a-axis and also gives rise to an increase of Cure temperature (from 360 K to 450 K). The average magnetic moments at all sites increase from 1.3 to 1.6  $\mu_B$ /atom at room temperature upon nitrogenation. We must mention that the statistical errors on the magnetic moment are quite large, as shown in the Table. Due to the difficulties in magnetic moment determination, the absolute value of the moment on each crystallographic site may not be very accurate, but definite conclusion can nevertheless be drawn, especially the influence of the interstitial N atom on the magnetic moments at different Fe sites. It is believed that the theoretical calculation results are more reliable based on true crystallographic structures of the  $\text{YFe}_{10}\text{Mo}_2$  and  $\text{YFe}_{10}\text{Mo}_2\text{N}_x$ .

### §3. Calculation Details

The LMTO method in atomic-sphere approximation (ASA) has been employed to perform a semi-relativistic band calculation in the frame of the local spin density (LSD) functional theory. Exchange and correlation term takes the form deduced by Von Barth and Hedin,<sup>22)</sup> with the parameter given by Janak.<sup>23)</sup> The s, p, and d orbitals are used for Y, Fe, Mo, and s, p orbitals are used for N atoms. The core charge densities and spin densities are calculated in each self-consistent procedure using relaxed core approximation. Convergence is assumed when the root-mean-square error of the self-consistent potential is better than 1mRy. The atoms sphere radii are chosen to be  $r_Y:r_{\text{Fe}}:r_{\text{Mo}}=1.35:1:1.12$  following ref. 12. Since the calculated results depend rather sensitively on the atomic-sphere radii, we choose atomic sphere radius ratio  $r_N/r_{\text{Fe}}=0.6$  according to ref. 7. The calculations are performed for 126 K points in the irreducible parts of the Brillouin zone. The atomic positions of  $\text{YFe}_{10}\text{Mo}_2$  and  $\text{YFe}_{10}\text{Mo}_2\text{N}$  are scaled according to our experimental results listed in Table I. We have done calculations when two Mo atoms occupy different two of the four 8i sites. The calculated magnetic moments of Fe atoms are

2.63, 2.04 and  $2.15 \mu_B$  for 8i, 8j and 8f sites, respectively, when two Mo atoms occupy positions (0.395, 0.0, 0.0), (-0.395, 0.0, 0.0), and the moments are 2.55, 2.02 and  $2.12 \mu_B$  for 8i, 8j and 8f sites when two Mo atoms occupy positions (0.395, 0.0, 0.0), (0.0, 0.395, 0.0). It is found that the difference is small. Thus, we select the case of (0.395, 0.0, 0.0), (-0.395, 0.0, 0.0) as a representation to simply study the interstitial nitrogen atoms effect. In order to elucidate the magneto-volume effect and chemical bonding effect of nitrogen atoms, we have performed four calculations.

(A)  $YFe_{10}Mo_2$  with the experimental lattice parameters of pure system.

(B)  $YFe_{10}Mo_2$  with the coordinates of pure  $YFe_{10}Mo_2$  scaled according to the experimental lattice constant of the nitrogenated compounds, but with an empty sphere (E) ( $r_E/r_{Fe}=0.6$ ) at 2b interstitial position. In the following we refer to this case by symbol  $YFe_{10}Mo_2E$ . This result represents the magneto-volume effect produced by the interstitial nitrogen atoms. So the difference between the results of (A) and (B) indicates the magneto-volume effect of nitrogen atoms.

(C)  $YFe_{10}Mo_2N$  with the coordinates of nitrides at the experimental lattice constants of  $YFe_{10}Mo_2N$ . The difference between the results of (B) and (C) shows the chemical bonding effect of the nitrogen atoms.

(D)  $YFe_{10}Mo_2N$  with a varying lattice constants and atomic position of  $YFe_{10}Mo_2N$ . We choose nine points for calculations and the volume variance between adjacent point is 20% of the volume expansion  $\Delta V$  from  $YFe_{10}Mo_2$  to  $YFe_{10}Mo_2N$ .

The Fermi-contact hyperfine fields ( $H_{FC}$ ) and isomer shifts ( $IS$ ) are calculated according to the prescription of Akai *et al.*<sup>24)</sup>

## §4. Results and Discussions

### 4.1 Electronic structures

In Fig. 2, we presented the total density of states (DOS) for cases  $YFe_{10}Mo_2$ ,  $YFe_{10}Mo_2E$  and  $YFe_{10}Mo_2N$ . A comparison of DOS between  $YFe_{10}Mo_2$  and  $YFe_{10}Mo_2N$  will give some information of total interstitial nitrogen atoms effect. It can be seen that the DOS of the alloy and nitride have a similar shape. However, there are mainly two pronounced differences in their DOS: (1) An isolated structure locates around  $-1.2Ry$  due to 2s states of N atoms in the DOS of  $YFe_{10}Mo_2N$ . (2) An additional structure at  $-0.6Ry$  below d bands comes from N 2p states, which also appears in the iron-nitrides<sup>25,26)</sup> and  $R_2Fe_{17}N_x$  compounds.<sup>6-8)</sup> The main structure around the Fermi-energy  $E_F$  is almost completely composed of 3d, 4s and 4p states of Fe atoms.

In Fig. 3, we presented the calculated s, p and d densities of the states of each atoms in the  $YFe_{10}Mo_2N$ . It is easy to see from the DOS that a similar structure appears in the DOS of Y(2a) and Fe(8j) at  $-1.2Ry$ . The appearance of these bonding states is due to the interaction among N(2b) s-state, Y(2a) states and Fe(8j) states. This can be more easily seen as we look the s-DOS at nitrogen given in the Fig. 3(f), since s-DOS has the significant values only in the range from  $-1.2Ry$  to  $-1.1Ry$ . The p-DOS of N shows pronounced peaks in the range 0.62–

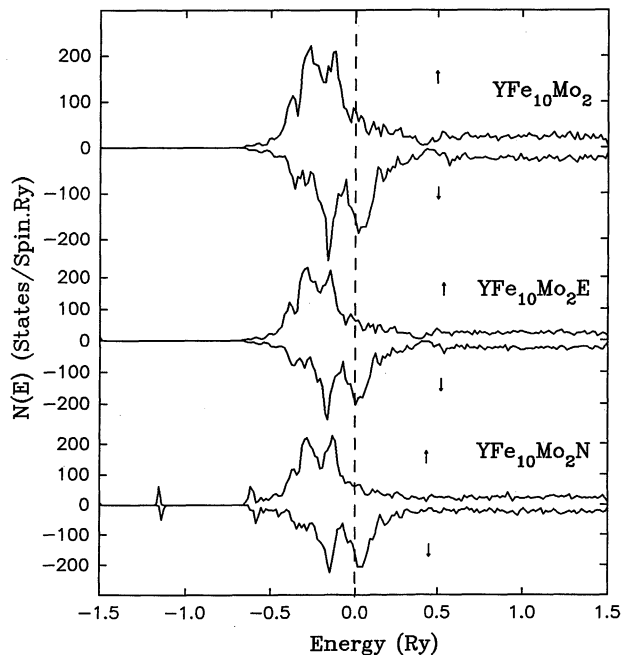


Fig. 2. Total densities of states of  $YFe_{10}Mo_2$ ,  $YFe_{10}Mo_2E$  and  $YFe_{10}Mo_2N$ .

$0.51Ry$  and a consequence of the interactions among N-2p states, Y(2a) and Fe(8j) states, we find these peaks in the same energy range in the DOS of the Y(2a) and Fe(8j) atoms. Thus we confirm that there is strong interaction between Y(2a) and N(2b) atoms, as well as Fe(8j) and N(2b) atoms. In contrast with the evidence of strong interaction between N and Fe(8j), the N-Fe(8i) and N-Fe(8f) cases are more subtle. An inspection of the Fig. 3 shows that there are no interaction between N s-states and the Fe(8i), as well as N s-states and Fe(8f) states. For the Fe(8j) s-DOS, we clearly see the existence of the bonding states which comes from the interaction between these states and N states. Also from the p-DOS, we notice the existence of a small interaction between p states of N and d states of Fe(8j). The d-DOS of Fe(8i) and Fe(8f) shows the absence of interaction between N p-states and their states.

### 4.2 Magneto-volume effect and chemical bonding effect of N atoms

The calculated results of  $YFe_{10}Mo_2$ ,  $YFe_{10}Mo_2E$  and  $YFe_{10}Mo_2N$  are shown in Fig. 4. The magneto-volume effect may be elucidated through a comparison between  $YFe_{10}Mo_2$  and  $YFe_{10}Mo_2E$ . By volume expansion, the local magnetic moments (Fig. 4(a)) and hyperfine fields (Fig. 4(b)) of different Fe sites are all increased in absolute value comparing to  $YFe_{10}Mo_2$ . The total increase of the magnetic moment due to the magneto-volume effect is about 4.7%. A comparison of the total DOS of  $YFe_{10}Mo_2$  and  $YFe_{10}Mo_2E$  shows that the expansion of unit cell volume will narrow the Fe-3d band and change the DOS at Fermi level  $E_F$ ,  $N_{E_F}$ . We decompose the hyperfine field  $H_{FC}$  into two contributions originating from core electrons ( $H_{FC}^{core}$ ) and valence electrons ( $H_{FC}^{val}$ ). As shown in Fig. 4(b), the  $H_{FC}^{core}$  is the dominated contribu-

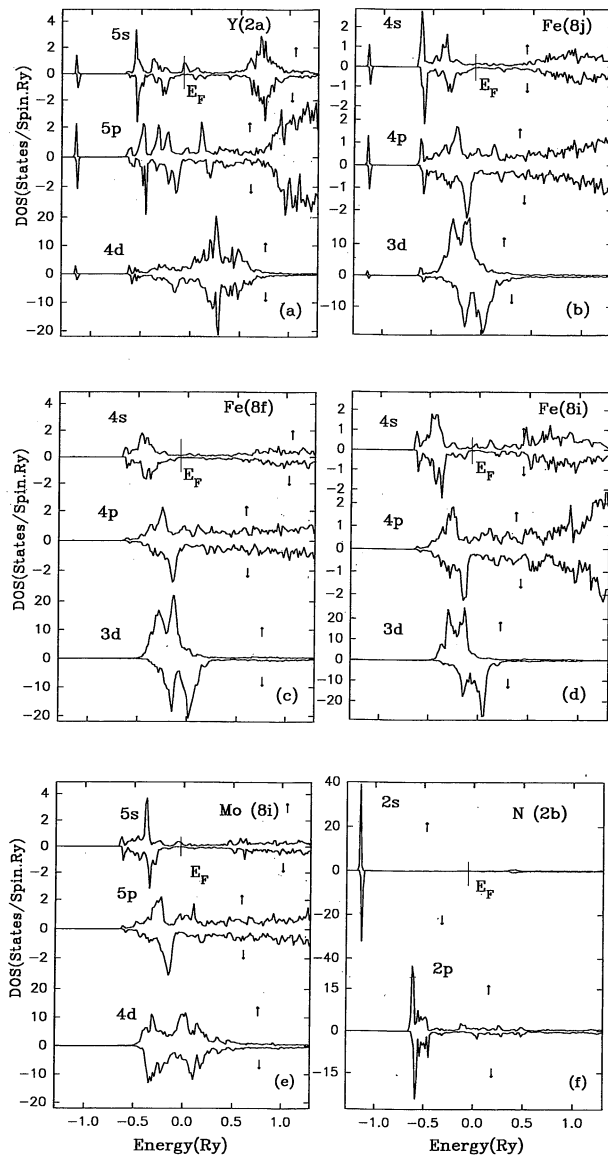


Fig. 3. The s, p and d densities of states for up and down states at different sites of  $YFe_{10}Mo_2N$ .

tion to  $H_{FC}$ . Figure 5 represents  $H_{FC}$  as well as their core and valence contributions as function to the local magnetic moments. Obviously, a linear relationship between  $H_{FC}^{core}$  and local magnetic moment at Fe sites is observed, and the proportional coefficient is estimated to be about  $-11.2T/\mu_B$ . Thus it can be seen that  $H_{FC}$  is affected by local magnetic moments of Fe and polarization valence contributions. Here we would like to point out that, since the experimental data on nitrides are rare, a thoroughly quantitative comparison is not available at the moment. Mössbauer study on these compounds at low temperature is required.

As listed in Table II, the electron number in  $YFe_{10}Mo_2$  and  $YFe_{10}Mo_2E$  indicates that there is charge transfer from spin-down states to spin-up states, as well as an increase of the population of the spin-up d-states due to the volume expansion, which will increase the magnetic moments and the hyperfine fields of Fe atoms.

Figure 4 also demonstrates the chemical bonding effect on the local magnetic moments and hyperfine fields.

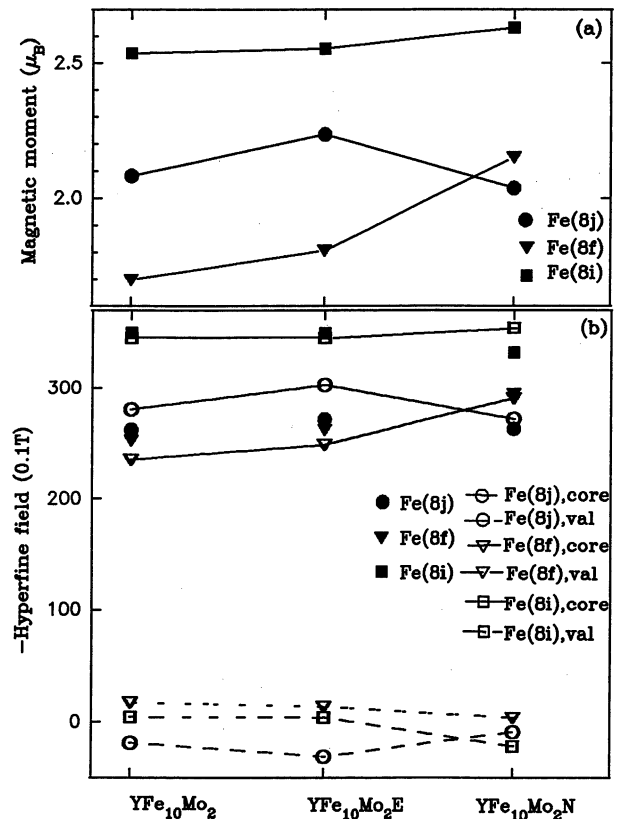


Fig. 4. The calculate results in  $YFe_{10}Mo_2$ ,  $YFe_{10}Mo_2E$  and  $YFe_{10}Mo_2N$ . (a) The local magnetic moments  $\mu_{Fe}$ . (b) The  $H_{FC}$  at Fe sites, and the core and valence contributions of  $H_{FC}$ .

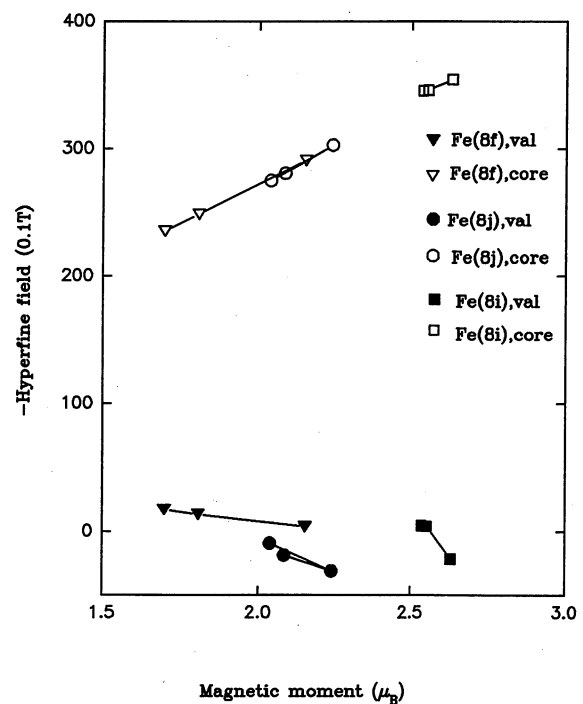


Fig. 5. The dependence of the  $H_{FC}^{core}$  and  $H_{FC}^{val}$  at Fe sites on the local magnetic moments  $\mu_{Fe}$  in  $YFe_{10}Mo_2$ ,  $YFe_{10}Mo_2E$  and  $YFe_{10}Mo_2N$ .

We present the data of  $YFe_{10}Mo_2E$  (B) (magneto-volume effect), together with those for  $YFe_{10}Mo_2N$  (C) (combination of magneto-volume effect and chemical bonding

Table II. Electron number and DOS at Fermi level  $N_{E_F}$  at different Fe sites in  $YFe_{10}Mo_2$ ,  $YFe_{10}Mo_2E$  and  $YFe_{10}Mo_2N$ .  $n$  is in electrons/spin, and  $N_{E_F}$  is in states/atom spin Ry.

	Sites	Orbital	$n\uparrow$	$n\downarrow$	$n\uparrow+n\downarrow$	$N(E_F)$
$YFe_{10}Mo_2$	Fe(8j)	3d	4.32	2.19	6.51	14.79
		4s	0.32	0.33	0.65	
		4p	0.35	0.40	0.75	
		total	4.99	2.92	7.90	
	Fe(8f)	3d	4.15	2.39	6.54	12.92
		4s	0.33	0.34	0.67	
		4p	0.39	0.45	0.84	
		total	4.87	3.18	8.05	
	Fe(8i)	3d	4.57	1.99	6.56	10.32
		4s	0.31	0.32	0.63	
		4p	0.33	0.37	0.70	
		total	5.21	2.68	7.89	
$YFe_{10}Mo_2E$	Fe(8j)	3d	4.40	2.11	6.51	15.88
		4s	0.32	0.32	0.64	
		4p	0.35	0.40	0.75	
		total	5.07	2.83	7.90	
	Fe(8f)	3d	4.21	2.33	6.54	12.82
		4s	0.33	0.34	0.67	
		4p	0.39	0.45	0.84	
		total	4.93	3.12	8.05	
	Fe(8i)	3d	4.58	1.98	6.56	12.39
		4s	0.31	0.32	0.63	
		4p	0.33	0.37	0.70	
		total	5.22	2.67	7.89	
$YFe_{10}Mo_2N$	Fe(8j)	3d	4.34	2.27	6.61	16.09
		4s	0.31	0.31	0.62	
		4p	0.40	0.43	0.83	
		total	5.05	3.01	8.06	
	Fe(8f)	3d	4.36	2.15	6.51	13.90
		4s	0.33	0.34	0.67	
		4p	0.38	0.43	0.81	
		total	5.07	2.92	7.99	
	Fe(8i)	3d	4.60	1.94	6.54	14.93
		4s	0.32	0.32	0.64	
		4p	0.33	0.36	0.69	
		total	5.25	2.62	7.87	

effect). Obviously, the chemical bonding effect will increase the magnetic moments of the Fe(8i) and Fe(8f) sites, but decrease that of Fe(8j) sites which are the nearest neighbor of N atoms. This result is in a good agreement with the neutron diffraction experiments.<sup>19)</sup> The decrease of the magnetic moments of Fe(8j) comes from two factors: an inversion of spin-up d-states into spin-down d-states, as well as the population of spin-down d-states at Fe(8j) sites by the excess electrons yielded by other Fe and N atoms. However, an inversion of spin-down d states into spin-up d states at Fe(8f) sites and population of spin-up d-states cause a large increase of the magnetic moments in Fe(8f) sites. The electron number at 8i sites is almost unchanged, so a little increase was found.

We can relate these results to the nearest neighbor (NN) environment in the crystal structure, namely, the ligand number and the nearest neighbor distances of the Fe atoms at different sites. The Fe(8j) and Fe(8f) have 8 NN irons, while Fe(8i) has 10.5 iron neighbor on average. The Fe–N distances are 1.93 Å, 3.27 Å, 3.93 Å for 8j, 8f, 8i sites, respectively, and Y(2a)–N distance is 2.40 Å. The shortest Fe(8j)–N distance causes a strong overlap

between N and Fe(8j) states, and the iron moments at 8j sites are severely reduced on account of N–Fe(8j) bond. On the other hand, two additional N atoms become the nearest neighbor of Y atoms. The hybridization between Y(2a) and N atoms forms a tight covalent bond, which would releases the surrounding Fe atoms from bonding with the Y atoms. This will give rise to an increase for the magnetic moments at Fe(8f) sites. As to Fe atoms at 8i sites, Fe–N distance and Fe–Fe NN number are larger than those of Fe atoms at 8f sites. The chemical bonding effects of N atoms will have little effect on 8i sites due to the fact that Fe–Fe interactions are dominate at these sites. The results confirm that total magnetic moment of the alloy will be further increased due to the N insertion without volume expansion. As a fact, the chemical bonding effect of the N insertion increases the total magnetic moment by about 4.1%.

The chemical bonding effect will decrease the Fe hyperfine fields of both 8j and 8i sites and increase that of 8f sites in absolute value.

Moreover, we can discuss the interstitial-atom effect on the isomer shifts. The calculated result is relative to that of  $\alpha$ -Fe with a calibrate constant  $\alpha = -0.24a_0^3 m \text{ msec}^{-1}$ . The calculated isomer shifts of the  $YFe_{10}Mo_2$ ,  $YFe_{10}Mo_2E$  and  $YFe_{10}Mo_2N$  are given in Fig. 6. It is obvious that the magneto-volume effect will increase the isomer shift due to the decrease of the charge density at Fe nucleus by volume expansion. The chemical bonding effect of the nitrogen increases the  $IS$  at all Fe sites. A large increase of  $IS$  was found in Fe(8j) sites, which indicates a strong hybridization between Fe(8j) and N atoms. This hybridization promotes the mobility of the electrons, and then in turn decrease the s-like charge density at the Fe nucleus, so the  $IS$  at Fe sites increase.

As function of the unit cell volume, the local magnetic moments (Fig. 7(a)) and hyperfine fields (Fig. 7(b)) at different Fe sites in  $YFe_{10}Mo_2N$  compounds are calculated, as shown in Fig. 7. The magnetic moments and hyperfine fields (absolute values) at different Fe sites increase monotonously with lattice expansion through the magneto-volume effect. In spite of the non-linear dependence of the magnetic moment at Fe sites on unit cell volume, we have used the formula

$$\ln \mu(V) = A + B \ln V \quad (1)$$

to fit the magnetic moments at Fe sites. The fitting results show that  $\partial \ln \mu_{Fe}^{8j} / \partial \ln V = 1.94$  for 8j sites,  $\partial \ln \mu_{Fe}^{8f} / \partial \ln V = 1.35$  for 8f sites, and  $\partial \ln \mu_{Fe}^{8i} / \partial \ln V = 0.90$  for 8i sites. For the average Fe magnetic moments, we also obtained  $\partial \ln \bar{\mu} / \partial \ln V = 1.70$ . For different Fe sites, the logarithmic volume derivative  $\partial |H_{FC}| / \partial \ln V$  is found to be 1.73, 1.19, and 0.76 for 8j, 8f and 8i sites, respectively, and  $\partial \ln |H_{FC}| / \partial \ln V = 1.28$ .

It is found that the Fe magnetic moments and hyperfine fields at 8i sites are more stable against the unit cell expansion than those at 8j and 8f sites.

Figure 8 presents the calculated volume dependence of  $IS$  at Fe sites in  $YFe_{10}Mo_2N$ . As shown in the figure, with increasing unit cell volume, the  $IS$  at Fe sites increase. The volume expansion will decrease s electron

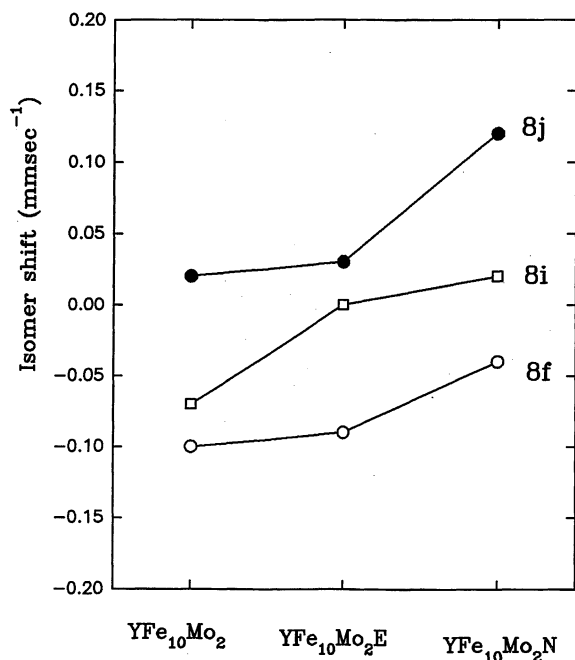


Fig. 6. The isomer shifts at different Fe sites in  $\text{YFe}_{10}\text{Mo}_2$ ,  $\text{YFe}_{10}\text{Mo}_2\text{E}$  and  $\text{YFe}_{10}\text{Mo}_2\text{N}$ .

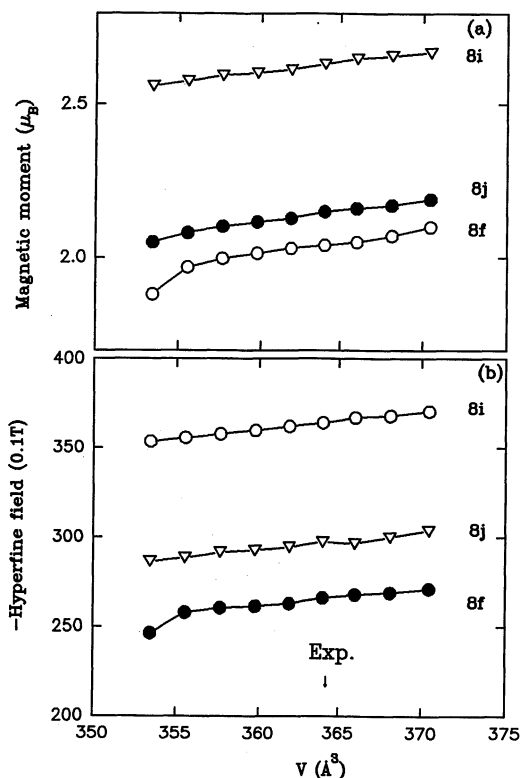


Fig. 7. The volume dependence of the (a) local magnetic moments and (b) hyperfine fields at different Fe sites of  $\text{YFe}_{10}\text{Mo}_2\text{N}$ .

density and s-d hybridization in  $\text{YFe}_{10}\text{Mo}_2\text{N}$  which decrease the charge density  $\rho(0)$  at the Fe nucleus, and so increase the  $IS$ . Fitting the variation of  $IS$  at Fe sites, we obtain  $\partial IS_{\text{Fe}}^{8j} / \partial \ln V = 2.00$  for 8j sites,  $\partial IS_{\text{Fe}}^{8f} / \partial \ln V = 1.99$  for 8f sites, and  $\partial IS_{\text{Fe}}^{8i} / \partial \ln V = 1.51$  for 8i sites. For the average isomer shift,  $\partial \overline{IS} / \partial \ln V = 1.90$ . This value

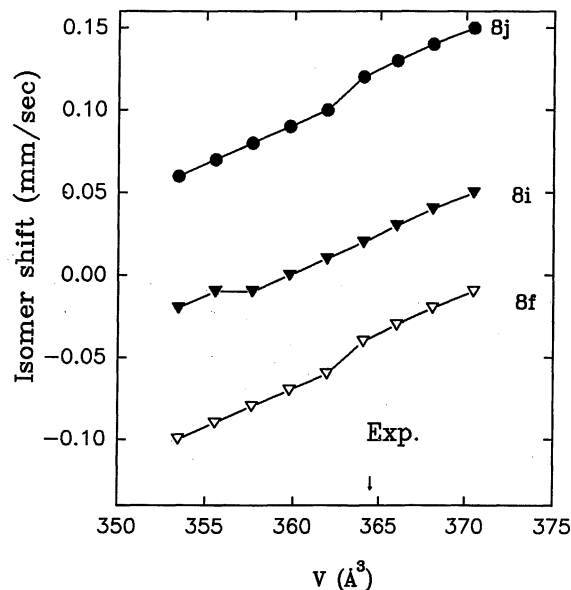


Fig. 8. The volume dependence of the isomer shifts at different Fe sites of  $\text{YFe}_{10}\text{Mo}_2\text{N}$ .

is close to that for  $\text{NdFe}_{10.5}\text{Mo}_{1.5}\text{N}_x$ .<sup>27)</sup>

## §5. Conclusions

We have presented a systematic study of the magnetic moments and hyperfine parameters of the  $\text{YFe}_{10}\text{Mo}_2$  and  $\text{YFe}_{10}\text{Mo}_2\text{N}$  by means of neutron diffraction measurement and LMTO-ASA method. The nitrogen atoms located at the 2b interstitial sites, which have a great effect on the magnetic properties of the 1:12 compounds. The nitrogenation modifies the Fe magnetic moments, particularly the individual moments on each crystallographic sites. It has been shown that there are mainly two effects of the N insertion, namely magneto-volume effect which absolutely increases the magnetic moment of each Fe site and total magnetic moment of the alloy, and the chemical effect which results in an enhanced moments on the 8i and 8f sites and a reduced moment on the 8j sites. And the chemical bonding effect will further increase the total magnetic moment of alloys. The magneto-volume effect will increase the absolute value of the hyperfine fields at three Fe sites. The chemical bonding effect will decrease the absolute values of Fe hyperfine fields in 8j and 8i sites, but increase that of 8f sites. It is found that the Fe magnetic moments and hyperfine field at 8i sites are more stable against the volume expansion than that at 8j and 8f sites. Both chemical bonding effect and magneto-volume effect will increase the  $IS$  at all Fe sites.

This work was supported by the National Natural Science Foundation and the National Target Basic Research Project.

- 1) J. M. D. Coey and H. Sun: *J. Magn. Magn. Mater.* **87** (1990) L251.
- 2) Y. C. Yang, X. D. Zhang, L. S. Kong, Q. Pan and S. L. Ge: *Appl. Phys. Lett.* **58** (1991) 2042.
- 3) H. Sun, J. M. D. Coey, Y. Otani and D. P. F. Hurley: *J. Phys.: Condens. Matter* **2** (1990) 6465.

- 4) Y. C. Yang, X. D. Zhang, L. S. Kong, Q. Pan, S. L. Ge, J. L. Yang, Y. F. Ding, B. S. Zhang, C. T. Ye and L. Jin: *Solid State Commun.* **78** (1991) 317.
  - 5) Q. N. Qi, H. Sun, R. Skomski and J. M. D. Coey: *Phys. Rev. B* **45** (1992) 12278.
  - 6) S. S. Jaswal, W. B. Yelon, G. C. Hadjipanayis, Y. Z. Wang and D. J. Sellmyer: *Phys. Rev. Lett.* **67** (1991) 644.
  - 7) T. Beuerle and Fähnle: *Phys. Status Solidi B* **174** (1992) 257.
  - 8) P. Uebele, K. Hummler and M. Fähnle: *Phys. Rev. B* **53** (1996) 3296.
  - 9) Y. P. Li and J. M. D. Coey: *Solid State Commun.* **81** (1992) 447.
  - 10) A. Sakuma: *J. Phys. Soc. Jpn.* **61** (1992) 4119.
  - 11) R. Coehoorn: *Phys. Rev. B* **41** (1990) 11790.
  - 12) I. A. Al-Omari, S. S. Jaswal, A. S. Fernando, D. J. Sellmyer and H. H. Hamdeh: *Phys. Rev. B* **50** (1994) 12665.
  - 13) J. Trygg, B. Johansson and M. S. S. Brooks: *J. Magn. Mater.* **104** (1992) 1447.
  - 14) W. Y. Hu, J. Z. Zhang, Q. Q. Zheng and C. Y. Pan: *J. Appl. Phys.* **76** (1994) 6751.
  - 15) S. Asano, S. Ishida and S. Fujii: *Physica B* **190** (1993) 155.
  - 16) S. Ishida, S. Asano and S. Fujii: *Physica B* **193** (1994) 66.
  - 17) O. K. Anderson: *Phys. Rev. B* **12** (1975) 3060.
  - 18) H. L. Skriver: *The LMTO Method*, ed. M. Cardona, P. Fulde and H. J. Queisser (Springer, Berlin, 1984).
  - 19) H. Sun, Y. Morij, H. Fujii, M. Akayama and S. Funahashi: *Phys. Rev. B* **48** (1993) 13333.
  - 20) F. Izumi: *The Rietveld Method*, ed. R. A. Yong (Oxford University Press, Oxford, 1993) Chap. 13.
  - 21) W. B. Yelon and G. C. Hadjipanayis: *IEEE Trans. Magn. MAG-28* (1992) 2316.
  - 22) U. von Barth and L. Hedin: *J. Phys. C* **5** (1972) 1629.
  - 23) J. F. Janak: *Solid State Commun.* **25** (1978) 53.
  - 24) H. Akai, M. Akai, S. Blügel, B. Drittler, E. Ebert, K. Terakura, R. Zeller and P. H. Dederichs: *Prog. Theor. Phys. Suppl.* **101** (1990) 11.
  - 25) A. Sakuma: *J. Magn. Mater.* **102** (1992) 127.
  - 26) C. A. Kuhnen, R. S. de Figueiredo and V. Drago: *J. Magn. Mater.* **111** (1992) 95.
  - 27) Q. N. Qi, B. P. Hu and J. M. D. Coey: *J. Appl. Phys.* **75** (1994) 6235.
-